Proceedings of the 6th International Conference on Recrystallization and Grain Growth (ReX&GG 2016) *Edited by: Elizabeth A. Holm, Susan Farjami, Priyadarshan Manohar, Gregory S. Rohrer, Anthony D. Rollett, David Srolovitz, and Hasso Weiland*
TMS (The Minerals, Metals & Materials Society), 2016

GRAIN REFINEMENT AND TEXTURE EVOLUTION IN HIGHLY DEFORMED FERRITE DURING HIGH-TEMPERATURE TORSION DEFORMATION OF IF STEEL

Reza Gholizadeh[1], Akinobu Shibata[1,2], Nobuhiro Tsuji[1,2]

[1]Department of Materials Science and Engineering, Kyoto University;
Sakyo-ku; Kyoto, 606-8501, Japan
[2]ESISM (Elements Strategy Initiative for Structural Materials), Kyoto University;
Sakyo-ku; Kyoto, 606-8501, Japan

Keywords: Grain Refinement, Interstitial Free Steel, Hot-Torsion Deformation, Texture

Abstract

Hot torsion test was employed to continuously deform an ultra-low carbon Ti-added interstitial free (IF) steel within a ferrite single-phase region (< 850°C) at different strain rates. Specimens were twisted to high equivalent strains up to 7.2 and immediately water-quenched to prevent post-deformation recrystallization. Microstructure observations were carried out near the surface of the torsion specimens using electron backscattered diffraction (EBSD) measurements. The results showed that the initial grains were elongated and subdivided, so that the distance between high angle boundaries (HABs) decreased with decreasing the temperature or with increasing the strain rate. It was believed that grain subdivision mechanism accompanied with dynamic recovery as well as limited boundary migration were responsible to the evolution of the microstructures. Furthermore, micro-texture measurements showed a strong development of <111> orientation parallel to the shear direction, among which, {112}<111> : {shear plane normal}<shear direction>, had a high fraction particularly within the low misorientation regions (LMRs).

Introduction

Metals with high stacking fault energy (SFE) are well-known for their easy-recovery ability in high-temperature deformations. As a result, the occurrence of conventional discontinuous dynamic recrystallization (dDRX), characterized by the nucleation (formation) of new dislocation-free grains and their growth into the deformed matrix, becomes difficult except for the case of high-purity metals. Ferritic (α-) iron is a typical example of this category in which flow stress in the high-temperature deformation shows a plateau with only a slight stress drop after a peak stress [1-4]. It has been generally accepted that dynamic recovery (DRV) is the main restoration mechanism in ferritic iron and steels. However, even in the hot deformation of high-SFE metals, new high angle boundaries (HABs) after relatively high strains form. The formation of new grain structures cannot be simply explained only by dynamic recovery. The development of HABs during the deformation of high-SFE metals has been tried to be explained by continuous dynamic recrystallization (cDRX) mechanism [5, 6]; that is the gradual change of subgrains into fine grains surrounded by HABs after a sufficient strain. However, many aspects of cDRX are still unclear and need to be clarified.
The aim of this study is to highly deform an ultra-low carbon interstitial free (IF) steel in a ferrite single-phase region (< 850 °C) under different deformation conditions for clarifying how the

microstructure evolution including the new grain formation occurs. Hot torsion is a popular deformation method to accurately control deformation conditions up to very high strains continuously. However, it has been proved [7, 8] that in the hot-torsion deformation of ferrite, certain texture components dominate at high strains at the cost of other orientations. Accordingly, it is also worth investigating how the texture formation in the hot-torsion deformed ferrite affects the microstructural evolution.

Experimental

A Ti-added IF steel with a fully recrystallized microstructure (mean grain size ~ 60 μm) in the as-received state and a chemical composition of 0.002 C, 0.01 Si, 0.12 Mn, 0.003 P, 0.003 S, 0.034 Ti, 0.028 Al, and 0.002 N (wt%) was used in this study. The initial bar material was machined into a cylindrical torsion specimen with a gauge part of 8 mm-diameter and 4 mm-length. To do the high-strain deformation at elevated temperatures, a series of free-end torsion tests were conducted at different temperatures (within a ferrite single-phase region; T < 850 °C) and strain rates (0.01 s^{-1} to 1 s^{-1}) in a thermomechanical processing simulator (Thermecmastor-TS). Firstly, the torsion specimen was heated up to a designed temperature and held at that temperature for 5 minutes for homogenizing the temperature. Then, the torsion deformation was carried out to different strain levels up to the maximum von-Mises equivalent strain of 7.2. Finally, water-quenching immediately after the deformation (less than 1 second) was used to stop post-dynamic recrystallization as much as possible. For the microstructure observations, a tangential section close to the surface (white rectangular in **Fig. 1**) of the gauge part of the torsion specimen was prepared by mechanical polishing and subsequent final polishing by a 0.04 μm colloidal silica suspension. Both microstructure and texture evolution were analyzed using Electron Back-scattering Diffraction (EBSD) measurements in a field emission scanning electron microscope (FE/SEM- JEOL JSM 7100F) operated at 15 kV. Furthermore, it should be noted that all microstructures provided in this paper indicate the torsion coordinate (θ, Z, r) illustrated in **Fig. 1**.

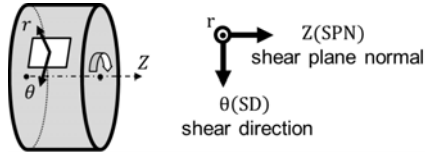

Figure 1. Gauge part of the torsion specimen with the tangential section (white rectangular) used for the microstructural observation; r is the radial direction perpendicular to the observed section, Z and θ are the shear plain normal direction and the shear direction, respectively.

Results and Discussion

Microstructure and texture evolution vs. strain

As explained in the previous section, the torsion specimens were deformed to different strain levels ($\varepsilon \leq 7.2$) under different test conditions. As an example, **Fig. 2** shows **(a)** an equivalent stress-

strain curve of the deformed IF steel under 750°C/0.01s^{-1} condition as well as **(b)-(d)** the corresponding microstructures at the strains of 0.3, 1.8, and 7.2. As expected, the flow stress of the hot-torsion deformed ferrite shows a typical flow curve of high SFE-metals; that is, a work hardening part until a peak stress followed by a slight stress drop (softening) and eventually a steady-state at high strains. The three EBSD HAB-boundary maps ($\theta \geq 15°$: shown by black lines) in **Fig. 2(b)-(d)** represent the evolved microstructures at hardening, softening, and steady-state stages, respectively. It should be mentioned that the hot deformed ferrite did not show a typical necklace-type DRX structure under any deformation conditions. Instead, it was observed that the formation of new grains occurred in an inhomogeneous way. As can be seen in **Fig. 2(b)** and **2(c)**, the initial microstructure became gradually elongated and subdivided (refined). The elongated HABs were directed toward the vertical direction; that is the shear direction (θ) shown in the right side of **Fig. 2**. The axis *a* shows the theoretical alignment (or major axis) of an elliptical grain after the corresponding simple shear deformation, assuming that the initial shape of the grain was a circle [9]. With further straining to the high strain of 7.2 (**Fig. 2(d)**), a type of structural coarsening occurred. Large areas with very few HABs inside (shown by arrows in **Fig. 2(d)**) or low misorientation regions (LMRs) could be clearly observed. Mean distance of high angle boundaries (d_{HAB}) as a parameter of grain refinement was plotted versus the equivalent strain in **Fig. 2 (e)**. This parameter firstly decreased from 55 μm to 19 μm and then increased to 25 μm at the high

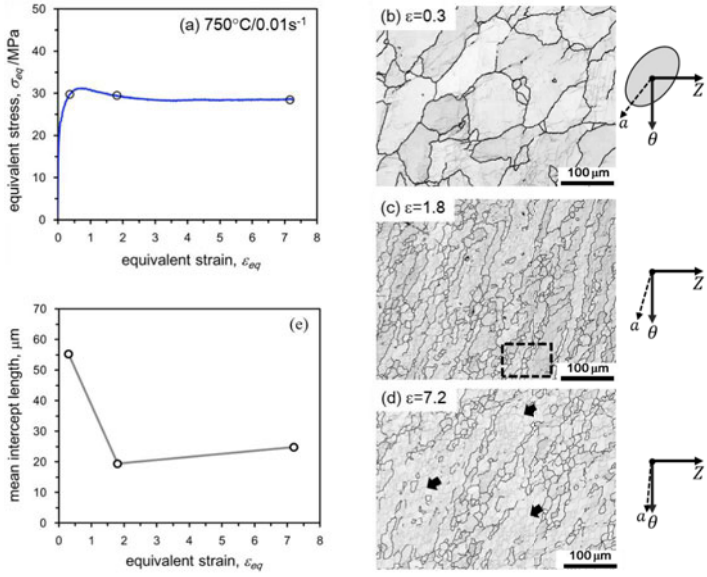

Figure 2. (a) Equivalent stress-strain curve of the IF steel hot-torsion deformed under the 750°C/0.01s^{-1} condition. (b, c, d) EBSD image quality/HAB-boundary maps of the IF steel specimens deformed under the 750°C/0.01s^{-1} condition to different strains, (b) $\varepsilon = 0.3$, (c) $\varepsilon = 1.8$, and (d) $\varepsilon = 7.2$. HABs with misorientations $\theta \geq 15°$ are drawn in black lines. (e) Diagram showing the mean distance of HABs versus the equivalent strain.

strain. An explanation for the structural coarsening with further straining is given later based on the development of torsion texture.

Moreover, to do a detailed investigation on the new grain structure at the middle of the softening stage ($\varepsilon = 1.8$), a rectangular area in **Fig. 2 (c)** (shown as a black frame) was chosen. **Figure 3** shows the EBSD orientation map of the same area. In this case, for the sake of discussion, boundaries are shown as thick black ($\theta \geq 15°$), thin black ($5° \leq \theta < 15°$) and thin grey lines ($2° \leq \theta < 5°$) for HABs, medium angle boundaries (MABs), and low angle boundaries (LABs), respectively. Elongated original grains were still detectable at this strain where grains were relatively serrated or bulged. The formation of the serrated boundaries is due to the interaction of grain boundaries with connected sub-boundaries, leading to the tension force at triple junctions and subsequent local boundary migration, which can be enhanced especially at higher deformation temperatures. Under the deformation conditions in this research, bulging of some boundaries (an initiation sign of dDRX) was observed to a limited extent although this could not be considered as a proof of dDRX or importance of this mechanism.

It could be seen that some segments of HAB and MAB (isolated or attached to the initial boundaries) formed within the deformed matrix. The formation of these new boundaries or so-called geometrically necessary boundaries (GNBs) can be explained by grain subdivision phenomena [10-12]; that is, different parts in a grain experiencing different slip patterns rotate in different directions and develop misorientations borne by GNBs. Average misorientation of GNBs gradually increases with straining and leads to fragmentation of grains into finer scales. Additionally, some new (sub-) grains mainly surrounded by HABs (marked by black arrows in **Fig. 3(a)**) also formed preferentially near the serrated grain boundaries. This may be related to certain strain accommodation patterns alongside the boundary affected zones. It is noteworthy that, in this study, the fragmentation of the deformed matrix were accelerated in the regions where the distance of original grain boundaries or deformation-induced boundaries became closer to form narrow zones. The misorientation distribution profile corresponding to the grain structure in **Fig. 3(a)** is also provided in **Fig. 3(b)**. As is suggested by the misorientation profile, a wide range of misorientations across the boundaries (a transition from low to medium and high angle boundaries) exists within the microstructure. Similarly, microstructures on many other sections were carefully examined. As a result, it could be concluded that the formation of new grain structure was basically attributed to the grain subdivision accompanied with dynamic recovery and limited boundary migration. It should be noted that in some literature [5, 6], hot-(or warm-) deformed

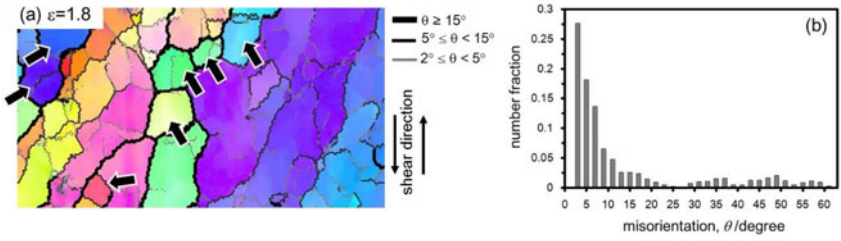

Figure 3. (a) EBSD orientation map of the area indicated by the rectangular frame shown in **Fig. 2(c)**. Boundaries are shown as thick black ($\theta \geq 15°$), thin black ($5° \leq \theta < 15°$) and thin grey lines ($2° \leq \theta < 5°$). (b) Misorientation profile in the corresponding microstructure.

microstructures of high-SFE metals have been discussed in terms of cDRX. In general, the cDRX phenomena have not yet been well understood and more investigations are necessary.
EBSD measurements were also used to analyze local texture of the deformed microstructures. **Figure. 4(a)** illustrates a schematic ODF plot at $\varphi_2 = 0°$ and $\varphi_2 = 45°$ sections in which important ideal orientations in torsion [8] are marked by different symbols. The notations used for different orientations and their Miller indexes with respect to the shear plane normal direction (Z) and the shear direction (θ) are shown in the table as well. The ODF sections corresponding to the microstructures shown in **Fig. 2(b)-(d)** are exhibited in **Fig. 4 (b)-(d)**. It is clear that with straining

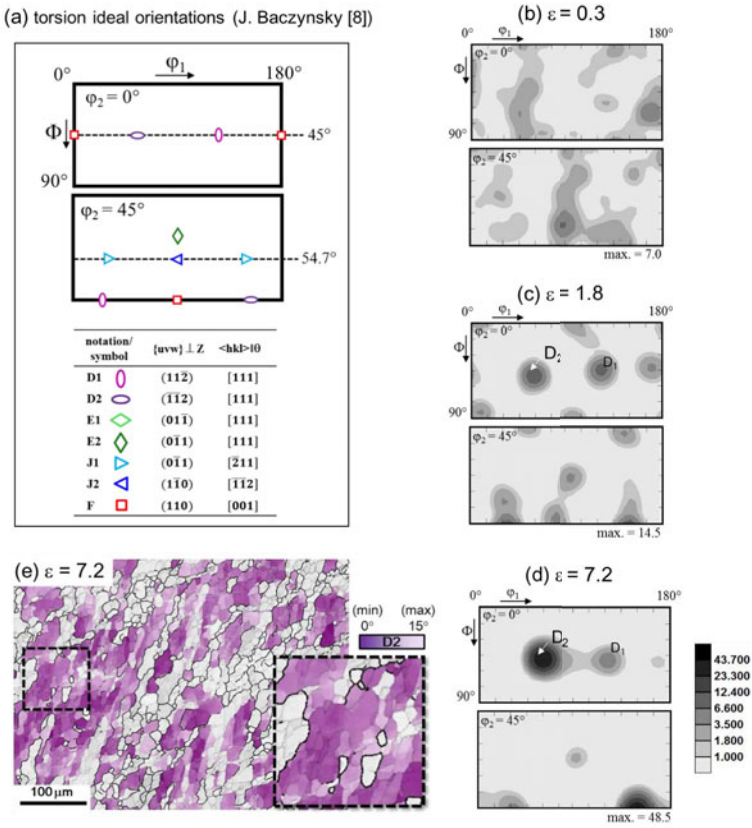

Figure 4. (a) Schematic ODF plot of φ_2=0° and φ_2=45° sections showing important ideal orientations in torsion as well as Miller notations [8]. (b, d, c) ODF sections of the specimens deformed under the 750°C/0.01s^{-1} condition to different strains: (b) ε = 0.3, (c) ε = 1.8, and (d) ε = 7.2. (e) Highlighted EBSD orientation map showing the intensities of D2 {$\bar{1}\bar{1}$2} <111> orientation in the specimen deformed to ε = 7.2 (the same area as **Fig. 2(d)**).

the ODF maps change from a relatively random texture pattern at the strain of 0.3 to a strong texture with the maximum intensities of 14.5 and 48.5 at the strains of 1.8 and 7.2, respectively. Texture measurements showed that at the medium strain (ε=1.8), D orientations; i.e., D1 $\{11\bar{2}\}$ <111> and D2 $\{\bar{1}\bar{1}2\}$ <111>, gradually became the major texture components. Other texture components having less intensities including E and F orientations also existed at this stage. It should be noted that except F, the D and E orientations belong to <111> ∥ θ type crystallography. With further straining to the high strain of 7.2, the D orientations (D2 in particular) developed to a great extent at the expense of other orientation components. The dominating D orientations were also found by macro-texture measurements of hot-torsion deformed IF steels [8], which was attributed to the formation of low-Taylor factor regions. The D (and E) orientations have the lowest Taylor factor among all ideal orientations in torsion. On the other hand, the development of a single end orientation (D2) at high strains can limit the grain refining process. In **Fig. 4 (e)**, D2-oriented regions were highlighted in the microstructure deformed to the strain of 7.2, which was the same area previously shown in **Fig. 2(d)**. The highlighted areas having the D2 orientation (with the tolerance angle of 15°) occupied approximately 55% (in area fraction) of the matrix and mainly formed the large LMRs with few high angle boundaries inside. Based on several observations in the present study, the development of the D2 regions seemed to be caused by a coalescence of D2-oriented clusters. Meanwhile, some high angle boundaries ($\theta \geq 15°$) disappeared with the development of the single-end texture resulting in an apparent structural coarsening as previously observed in **Fig. 2(d)**, leading to the limitation on the grain refinement.

Effect of deformation temperature and strain rate

To study the effect of deformation conditions, the torsion specimens were deformed to a certain strain at different temperatures and strain rates; i.e., under different Zener-Hollomon parameter ($Z = \varepsilon' \exp(Q/RT)$) conditions. **Figure 5(a)-(c)** show the effect of increasing Z parameter on the microstructural evolution. The amount of strain ($\varepsilon = 7.2$) is the same in all cases. It can be clearly seen that the grain refinement was enhanced by increasing the strain rate from $0.01 s^{-1}$ (**Fig. 5(a)**) to $1.0\ s^{-1}$ **(Fig. 5(b))** at 750°C, or decreasing the deformation temperature from 750°C (**Fig. 5(b)**) to 650°C (**Fig. 5(c)**) at a constant strain rate of $1.0\ s^{-1}$. In other words, with increasing the Z, the microstructural refining due to the grain subdivision occurred in a way that the mean distance of HABs decreased from 25 μm to 8 μm and 1.7 μm, respectively. Another consequence resulted from increasing Z is that HABs are apparently more elongated (e.g., **Fig. 5(c)**) toward the shear direction (θ). However, HABs seem more serrated but less inclined under the lower Z condition (e.g., **Fig. 5(a)**). One possible reason for this might be an enhanced mobility of HABs under the lower Z conditions since the boundary migration can counteract the elongation effect.
Figure 5(d)-(f) represent ODF maps of the corresponding microstructures shown in **Fig. 5(a)-(c)**. As previously discussed, a high intensity of D2 orientation was observed under the $750°C/0.01 s^{-1}$ condition in **Fig. 5(d)**. Similarly, the existence of D2 orientation was found in the other highly deformed specimens in **Fig. 5(e)** and **5(f)**. However, with increasing the Z parameter, the maximum intensities in the ODF plots decreased from 48.5 to 35 and 16, respectively. Regarding the fact that the amount of strain was the same in all cases, it could be concluded that the development of the D2 texture was retarded under the higher Z conditions.

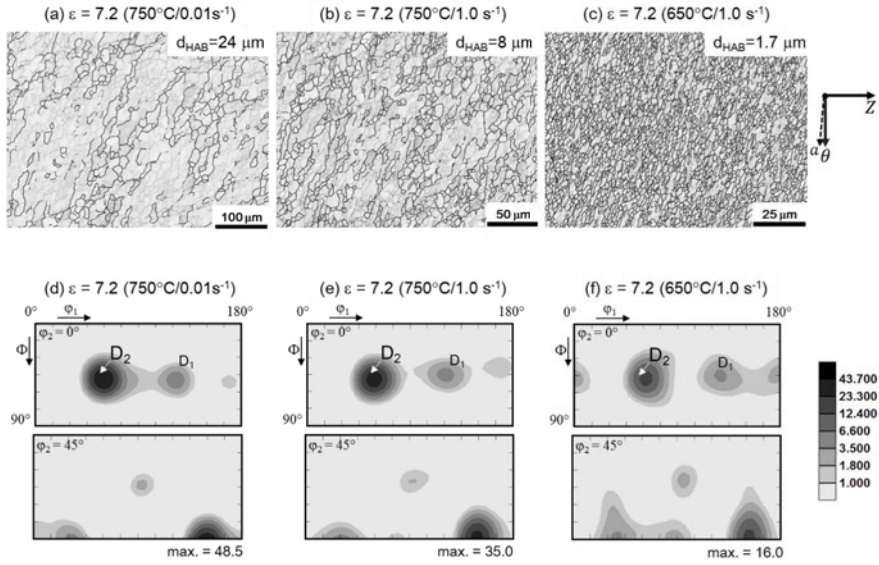

Figure 5. EBSD image quality/HAB-boundary maps of the IF steel specimens deformed to the strain of 7.2 under (a) 750°C/0.01s^{-1}, (b) 750°C/1.0 s^{-1}, and (c) 650°C/1.0 s^{-1} conditions. (d)-(f) ODF sections of the corresponding microstructures, respectively.

Conclusions

An IF steel was highly deformed within a ferrite single-phase region by a free-end hot-torsion test. The results showed that the initial grain structures were refined during the deformation by grain subdivision through the formation of GNBs as well as the formation of new fine (sub-) grains surrounded by HABs. Additionally, the increase in the Z values led to the enhancement of the refinement process while the new grain structures were more elongated toward the shear direction. On the other hand, the results of texture measurements showed that D2 $\{\bar{1}\bar{1}2\}$ <111> orientation, dominated in the hot-torsion deformed IF steel particularly under the lower Z conditions and high strains. The development of large D2-oriented regions with few HABs inside led to an apparent structure coarsening at high strains.

Acknowledgements

This study was financially supported by the Grant-in-Aid for Scientific Research (S) (No.15H05767), the Grant-in-Aid for Scientific Research on Innovative Area, "Bulk Nanostructured Metals" (area No.2201), and the Elements Strategy Initiative for Structural Materials (ESISM) all through the Ministry of Education, Culture, Sports, Science and Technology (MEXT), Japan. The supports are gratefully appreciated by the authors. R.G. gratefully thanks the

Japan Ministry of Education, Culture, Sports, Science and Technology (MEXT) for providing a Monbukagakusho scholarship.

References

1. G. Glovers and C.M. Sellars, "Recovery and Recrystallization during High Temperature Deformation of α-Iron," *Metallurgical Transaction*, 4 (1973), 765-775.

2. N. Tsuji, Y. Matsubara, and Y. Saito, "Dynamic Recrystallization of Ferrite in Interstitial Free Steel," *Scr. Mater.*, 37 (1997), 477-484.

3. C. Huang et al., "Flow Stress Modeling and Warm Rolling Simulation Behavior of Two Ti-Nb Interstitial-Free Steels in The Ferrite Region," *Acta Mater.*, 49 (2001), 1445-1452.

4. A. Oudin, P.D. Hodgson, and M.R. Barnett, "EBSD Analysis of A Ti-IF Steel Subjected to Hot Torsion," *Mater. Sci. and Eng.*, 486A (2008), 72-79.

5. S. Gourdet and F. Montheillet, "A Model of Continuous Dynamic Recrystallization," *Acta Materialia*, 51 (2003), 2685-2699.

6. T. Sakai et al., "Dynamic and Post-Dynamic Recrystallization under Hot, Cold and Severe Plastic Deformation Conditions," *Prog. Mater. Sci.*, 60 (2014), 130-207.

7. F. Montheillet, M. Cohen, and J.J. Jonas, "Axial Stress and Texture Development during The Torsion Testing of Al, Cu, α-Fe," *Acta Metall.*, 32 (1984), 2077-2089.

8. J. Baczynsky and J.J. Jonas, "Torsion Texture Produced by Dynamic Recrystallization in α-Iron and Two IF Steels," *Metallurgical and Materials Transactions*, 29A (1998), 447-462.

9. G.R. Canova, U.F. Kocks, and J.J. Jonas, "Theory of Torsion Texture Development," *Acta Metall.*, 32 (1984), 211-226.

10. D. Kuhlmann-Wilsdorf and N. Hansen, "Geometrically Necessary, Incidental and Subgrain Boundaries," *Scr. Metall. Mater.*, 25 (1991), 1557-1562.

11. D.A. Hughes and N. Hansen, "High Angle Boundaries Formed by Grain Subdivision Mechanisms," *Acta Mater.*, 45 (1997), 3871-3886.

12. N. Hansen, "New Discoveries in Deformed Metals," *Metall. Mater. Trans.*, 32 A (2001), 2917-2935.